Dilute suspension of small triaxial particles in shear: angular particle dynamics and suspension rheology

G. Almondo,[1, a)] J. Einarsson,[1, a)] J. R. Angilella,[2] and B. Mehlig[1]
[1)] *Department of Physics, University of Gothenburg, 41296 Gothenburg, Sweden.*
[2)] *LUSAC, Université de Caen, Cherbourg, France.*

(Dated: 19 July 2015)

We show numerical results for the orientational distribution of Brownian asymmetric ellipsoids in a simple shear flow. Results are obtained with a Langevin simulation and used to compute the viscosity of dilute suspensions of small ellipsoidal particles of various shapes in different noise regimes. The suspension shows shear dependent intrinsic viscosity similarly to asymmetric ellipsoids. We find that the suspension viscosity at low noise is nearly insensitive on particle shape.

general principles:
- all underlying physical principles, assumptions, and mechanisms must be explained, and how they result in the equations quoted. mathematical details are not needed. but a reader unfamiliar with suspension rheology must be able to understand the logical steps and the underlying physics.
- no sentence can be copied from other papers or your thesis.

I. INTRODUCTION

This article aims at characterising the rheological properties of a dilute suspension of small tri-axial rigid particles of ellipsoidal shape immersed in a simple shear flow. The presence of rigid particles in a fluid has been linked, since the pioneering work of Einstein[1,2], to new rheological properties of the suspension. In particular Einstein showed that a Newtonian fluid with a small quantity of small spherical particles suspended in it has a higher viscosity. The excess viscosity due to the suspended particles is proportional to the solution concentration. With the assumption that the suspension is infinitely diluted and therefore there is no interaction between particles, the statistical properties of a suspension can be determined by considering a single particle suspended in the ambient flow. Particles with central symmetry exhibit decoupled rotational and translational dynamics[3]. Here we only consider rotational dynamics. Ignoring effects due to particle and fluid inertia, the hydrodynamic stresses at the particle-fluid interface result in an angular velocity[4] proportional to the local gradient of the undisturbed flow. The particle's angular velocity depends in a nonlinear fashion on the instantaneous orientation of the particle. This inherent nonlinearity gives rise to complex behaviours, in which quasi-periodic[5,6] and chaotic[6] regimes have been identified, depending on the shape and initial orientation of the particle. Because of their small linear dimensions the particles are affected by the thermal fluctuations in the fluid, whose inherently stochastic nature gives rise to a diffusive process, known as rotational Brownian motion[7]. The competition between the hydrodynamic (deterministic) and the stochastic processes leads to a time-dependent orientational probability distribution, which shows a long-term steady state independent on the initial condition. Brownian motion has been identified as an important physical process involved in the determination of the rheological properties of the suspension. In particular the rheology of a dilute suspension can be found from the orientational distribution[8,9]. The presence of axisymmetric particles in the fluid has been shown to give rise to shear-dependent, non-Newtonian behaviour: numerical and analytical results have been obtained in the limit of vanishing[10], intermediate[11,12] and dominant[13] flow strength. Knowledge of the rheology of asymmetric ellipsoids is to date limited to the case of zero[14] and linear[15] flow strength.
In the present work we address the following questions:

- How does a triaxial ellipsoid rotate under the influence of the hydrodynamic and Brownian stresses at the surface of the particle?

[a)] These authors contributed equally to this work.

- What is the viscosity of a dilute suspension of such particles in a simple shear flow in presence of finite noise levels?

A Langevin-type stochastic simulation is employed to obtain the steady-state orientational distribution of an ensemble of identical particles. The distribution is then employed to evaluate the relevant rheological properties of the dilute suspension.

Organization of article

II. METHOD

The rheological properties of a dilute suspension are determined by the orientational dynamics of the suspended particles. The properties are embodied by the stress tensor associated with the suspension, averaged over the ensemble of all the possible orientations. In particular, the viscosity of a solution in a simple shear flow is defined as the scalar coefficient of proportionality between the component of the average stress tensor $\bar{\sigma}$ along the shear direction and the shear rate s (or as the average work per volume divided by the squared shear rate). Two contributions to the average stress tensor have been identified: one (direct) contribution arising from an effective angular velocity brought about by the Brownian diffusion. The indirect contribution results from the orientation distribution affecting the average sestresslet[8].

A. Particle dynamics

In the present work the ambient flow is $u_i^\infty = syx_i$, where s is called *shear rate*. The model particle is an ellipsoid with surface $x^2/a_1^2 + y^2/a_2^2 + z^2/a_3^2 = 1$. Without loss of generality we only consider $a_1 \geq a_2 \geq a_3$. The primary and secondary particle aspect ratios are $\lambda = a_1/a_3$ and $\kappa = a_2/a_3$, out of which two dimensionless "shape parameters" are defined as $\Lambda = (\lambda^2-1)/(\lambda^2+1)$ and $K = (\kappa^2-1)/(\kappa^2+1)$. The orientation of the particle is represented by a set of orthonormal axes $(\boldsymbol{n}, \boldsymbol{p}, \boldsymbol{q})$ rotating with the particle, and fixed on the particle's principal semi-axes respectively of length (a_1, a_2, a_3). At times we choose to use different parametrizations of rotations. For instance, results are shown with the help of Euler angles (ϕ, θ, ψ) because of their low dimensionality.

Because of the inherent algebraic difficulties entailed by Euler angles, we choose to reperesent the particle's orientation in terms of a rotation matrix $\mathbb{R}$ wich transforms a vector from particle to laboratory frame as $\omega_i = R_{i\alpha}\omega_\alpha$. The columns of $\mathbb{R}$ are the vectors (n, p, q) expressed in laboratory frame. Here and throughoutout we express tensors in index notation, with the understanding that Latin indices are used for quantities expressed in laboratory frame and Greek indices are used for quantities in particle frame.

Avoid. If necessary, explain better

avoid if possible. Leave it for now and change later.

The orientation dynamics of a rigid rotor is completely characterised by the dynamical equation

$$\dot{R}_{i\alpha}\left(R_{k\alpha}(t), t\right) = \epsilon_{ijk}\omega_j(t)R_{k\alpha}(t)\,, \tag{1}$$

where ω_j are the components of the angular velocity of the particle. At low Reynolds number the angular velocity is found to be linearly proportional to the ambient flow and to the torque imposed by the fluid. This linear proportionality, obtained by solving the Stokes equation at the boundary between particle and fluid, takes the name of generalized Faxén laws. Further, if the particle is light enough (vanishing Stokes number) one can impose that the total torque acting on the particle is null, thus finding that the angular velocity depends on the gradient of the ambient flow $\mathbb{A}^\infty$. Defined the symmetric $\mathbb{S}^\infty$ and antisymmetric $\mathbb{O}^\infty$ parts of the flow gradient as $\mathbb{A}^\infty = \mathbb{S}^\infty + \mathbb{O}^\infty$, as well as the vector $\Omega_i^\infty = -\epsilon_{ijk}O_{jk}^\infty$, the components of the hydrodynamic angular velocity computed by Ref. [4] are

$$\omega_i^H = \Omega_i^\infty + K(p_j S_{jk}^\infty q_k)n_i - \Lambda(q_j S_{jk}^\infty n_k)p_i + \frac{K-\Lambda}{K\Lambda-1}(n_j S_{jk}^\infty p_k)q_i\,. \tag{2}$$

The hydrodynamic equation has the following physical interpretation: the particle experiences separately the two contributions to the flow gradient: the rotational flow imparts a rigid body rotation to the particle, while the straining flow tends to "pull" the particle along the elongating direction. A sphere in a simple shear flow ($K = \Lambda = 0$), for example, rotates on itself with angular velocity equal to half that of the vorticity vector. A symmetric ellipsoid is also affected by the pull of the straining flow. The competition between the pull and the rotation determines a family of periodic trajectories named "Jeffery orbits" after Jeffery who first described them[4]. The motion of triaxial ellipsoids is complicated: depending on the initial condition, particles exhibit quasi-periodic[5] and chaotic[6] behaviour. In recent years the Jeffery equation has been put to the test with experiments[17], and is object of ongoing research.

The particles we consider are small enough to be affected by the thermal fluctuations in the fluid. The physical picture is the following: the particle is a rigid rotor suspended in a fluid, occasionally receiving an impulsion from the collision with a fluid molecule. The sum of a great quantity of small randomly directed impulsions imparts a random angular momentum to the particle. At the same time, the fluid exherts a viscous drag (torque) to oppose the motion of the particle. The combination of the viscous dampening and random torques gives rise to a constant rotational movement with random angular velocity $\boldsymbol{\omega}^D$ superimposed to the hydrodynamic angular velocity (2). In the following we derive the prescribed statistics of the random angular velocity.

Let us denote with $\boldsymbol{\Gamma}$ the random torque exherted on the particle by the thermal agitation in the fluid. The angular momentum exherted by the fluid to oppose the motion of the suspended particle is clearly $L_i = -I_{ij}\omega_j^D$, where $\mathbb{I}$ is the particle inertia tensor and $\boldsymbol{\omega}^D$ the particle's angular velocity due to the diffusion process. Because the Reynolds number of this motion is vanishingly low, we can make use of the generalized Faxén laws expressing the linear relation between the particle's relative angular velocity and the hydrodynamic torque $T_i = K_{ij}\omega_j^D$, $\mathbb{K}$ being the angular resistance tensor[18]. The orientational dynamics of the particle is described by the Langevin equation

$$\dot{L}_i = -K_{ij}\mathbb{I}^{-1}_{jk}L_k + \Gamma_i\,. \tag{3}$$

Possible notation conflict between shape factor K and angular resistance tensor $\mathbb{K}$

Like (1), eq. (3) is not defined if Γ is white noise. For the following derivation we need not assume that noise is white.

On average the work done by the random torque to move the particle is proportional to the temperature of the fluid T and the Boltzmann constant k_B, according to the equipartition theorem:

$$\langle L_i\omega_j^D\rangle = k_\mathrm{B}T\delta_{ij}\,. \tag{4}$$

The statistics of the random torque $\boldsymbol{\Gamma}$ are found by imposing the energy dissipation condition (4):

$$\langle\Gamma_i(t_1)\Gamma_j(t_2)\rangle = 2k_BTK_{ij}\delta(t_1-t_2)\,, \tag{5}$$

from which descend the statistics of the angular momentum $\boldsymbol{L}$:

$$\langle L_i\rangle = 0\,, \tag{6a}$$

$$\langle L_i(t_1)L_l(t_2)\rangle = k_BTI_{ij}e^{-K_{jk}\mathbb{I}^{-1}_{kl}|t_1-t_2|}\,. \tag{6b}$$

Finally, the correlation of the Brownian angular velocity[7] is:

$$\langle\omega_i^D(t)\rangle = 0\,, \tag{7a}$$

$$\langle\omega_i^D(t_1)\omega_j^D(t_2)\rangle = k_BT\mathbb{I}^{-1}_{ij}e^{-K_{jk}\mathbb{I}^{-1}_{kl}|t_1-t_2|}\,. \tag{7b}$$

We can take the weak limit for $\mathbb{I}\mathbb{K}^{-1}\to 0$ of the above to obtain

Here comes over-damped limit. Is this how it goes?

$$\langle\omega_i^D(t)\rangle = 0\,, \tag{8a}$$

$$\langle\omega_i^D(t_1)\omega_j^D(t_2)\rangle = 2DM_{ij}\delta(t_1-t_2)\,. \tag{8b}$$

having identified the diffusion constant $D = k_B T/6\eta V$ and in $\mathbb{M} = 6\eta V \mathbb{K}^{-1}$ the mobility tensor[14] defined in Appendix C, proportional to the inverse of the Stokes resistance tensor $\mathbb{K}$ coupling angular velocity and torque, which is found by solving the Stokes equation at the boundary of the particle. V is the volume of the particle.
The orientation is best described in terms of a distribution P governed by the continuity equation for the probability current in the space of orientations. The probability current has two contributions: one is given by the deterministic orientational dynamics, while the other results from the diffusion process embodied by a diffusion tensor proportional to the probability gradient.
Here we derive the continuity equation following Ref. [19] from the diffusion coefficients resulting from the microscopic stochastic dynamics:

$$\lim_{\delta t \to 0} \frac{\langle \delta R_{i\alpha} \rangle}{\delta t}\,, \tag{9a}$$

$$\lim_{\delta t \to 0} \frac{\langle \delta R_{i\alpha} \delta R_{j\beta} \rangle}{\delta t}\,. \tag{9b}$$

Generally speaking equation (1) is not defined if $\boldsymbol{\omega}$ is Gaussian noise, and therefore the latter should be supposed to be a well-behaved function with correlation time τ and finite width σ i.e. not delta-correlated. By formally letting $\tau \to 0$ while keeping a constant τ/σ one recovers a delta-correlated function.

The average angular displacement is derived as a first order expansion in δt from the dynamical equation for the orientation (1) $\boldsymbol{\omega}$ is a random function embodying thermal noise, with delta correlation in time. The displacement after a short time δt is readily found as

$$\begin{aligned}
\langle \delta R_{i\alpha} \rangle &= \langle R_{i\alpha}(\delta t) - R_{i\alpha}(0) \rangle = \int_0^{\delta t} \mathrm{d}t_1 \langle \dot{R}_{i\alpha} \left(R_{k\alpha}(t_1), t_1 \right) \rangle \\
&= \int_0^{\delta t} \mathrm{d}t_1 \langle \dot{R}_{i\alpha} \left(R_{k\alpha}(0) + \int_0^{t_1} \mathrm{d}t_2 \dot{R}_{k\alpha} \left(R_{l\alpha}(t_2), t_2 \right), t_1 \right) \rangle \\
&\approx \int_0^{\delta t} \mathrm{d}t_1 \langle \dot{R}_{i\alpha}(R_{k\alpha}(0), t_1) \rangle + \int_0^{\delta t} \mathrm{d}t_1 \int_0^{t_1} \mathrm{d}t_2 \langle \partial_{j\beta} \{ \dot{R}_{i\alpha} \left(R_{k\alpha}(t_1), t_1 \right) \} \dot{R}_{j\beta}(R_{l\beta}(t_2), t_2) \rangle\,,
\end{aligned} \tag{10}$$

wherein the last step we performed a first order Taylor expansion. Similarly one can obtain the average second displacement

$$\langle \delta R_{i\alpha} \delta R_{j\beta} \rangle = \int_0^{\delta t} \mathrm{d}t_1 \int_0^{\delta t} \mathrm{d}t_2 \langle \dot{R}_{i\alpha}(R_{k\alpha}(t_1), t_1) \dot{R}_{j\beta}(R_{l\beta}(t_2), t_2) \rangle\,. \tag{11}$$

The diffusion coeffients are readily computed by inserting (8) in (10) and (11), and finally in (9):

$$\lim_{\delta t \to 0} \frac{\langle \delta R_{i\alpha} \rangle}{\delta t} = D(M_{ij} R_{j\alpha} - M_{kk} R_{i\alpha})\,, \tag{12a}$$

$$\lim_{\delta t \to 0} \frac{\langle \delta R_{i\alpha} \delta R_{j\beta} \rangle}{\delta t} = 2D M_{kp} \epsilon_{ikl} \epsilon_{jpq} R_{\alpha l} R_{\beta q}\,, \tag{12b}$$

Finally the diffusion equation comprising of the deterministic velocity is[14]

$$\partial_t P = -\nabla_i \left[(\omega_i^H - D M_{ij} \nabla_j) P \right]\,. \tag{13}$$

where ∇ is the differential operator defined on the space of rotation matrices[14] as

$$\nabla_i = \epsilon_{ijk} R_{j\alpha} \partial_{k\alpha}\,. \tag{14}$$

in which $\partial_{k\alpha}$ is the usual Euclidean differential operator on the space of 3×3 matrices. The particular form of the differential operator is imposed by the necessity that the infinitesimal rotation matrix be in the same space of unitary orthogonal matrices, and descends naturally from the dynamical equation (1).

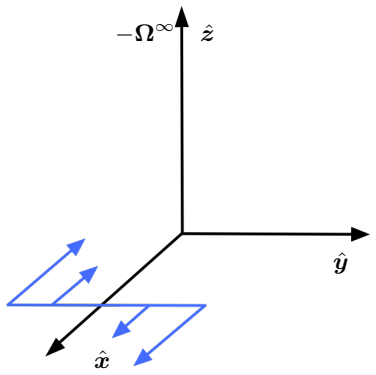

FIG. 1. Schematic diagram of the simple shear flow in coordinate system translated with the center of mass of the particle. Shown in the picture are the laboratory frame of reference $(\hat{\boldsymbol{x}}, \hat{\boldsymbol{y}}, \hat{\boldsymbol{z}})$, the vector $\boldsymbol{\Omega}^{\infty}$ and the direction the of gradient (blue straight line).

The diffusion equation (13) holds for any choice of parametrization of the space of orientations: each parametrization results in a specific differential operator ∇. In the present work we seek a numerical solution of the steady-state diffusion equation. To this end we choose to parametrize orientations with quaternions (see Appendix A for definitions and derivation), for which the diffusion equation is derived

can rewrite eq. 16 with lab-fixed ω^H, M_{ij} and diff. operator if needed. This could allow us to avoid Greek letters for body frame components

$$\partial_t P = -\frac{1}{2} G^i_\alpha \partial^i \omega^H_\alpha P + \frac{1}{4} D G^i_\alpha \partial^i M_{\alpha\beta} G^j_\beta \partial^j P \,, \tag{15}$$

where ω_α and $M_{\alpha\beta}$ are the components respectively of the hydrodynamic angular velocity and mobility matrix expressed in body frame. The matrix $\mathbb{G}$, defined in Appendix A, has the role of a projector operator from the quaternion space to the usual three dimensional Eucldean space. It embeds the special topology of the quaternion space. ∂^i are the components of the four dimensional Euclidean differential operator.
A steady state solution is found by means of the equivalent Langevin equation for quaternions $q^i(t+\delta t) = q^i(t) + \delta q^i(t)$, with

$$\delta q^i = \frac{1}{2} G^i_\alpha \omega^H_\alpha \delta t + \delta \xi^i(t) \,, \tag{16}$$

in which $\delta\boldsymbol{\xi}$ is a random vector in the four dimensional Euclidean space whose components have the same statistics as the diffusion coefficients of the diffusion equation for quaternions (see Appendix A):

$$\langle \delta \xi^i \rangle = -\frac{1}{4} D M_{kk} q^i \delta t \,, \tag{17a}$$

$$\langle \delta \xi^i \delta \xi^j \rangle = \frac{1}{2} D G^i_\alpha M_{\alpha\beta} G^j_\beta \delta t \,. \tag{17b}$$

B. Rheological properties

Consider a sphere of radius r and surface S_0 enclosing a Newtonian fluid containing N particles. The fluid is set in motion by a simple shear flow. Because the fluid is viscous, some energy is dissipated in the shearing process, according to the microscopic picture of viscosity. The presence of the particles creates an additional dissipation. The shear viscosity of a suspension can be defined as the volumetric density of work per square shear rate, i.e.

$$\eta' = W s^{-2} \,. \tag{18}$$

The mechanical work per volume (V_0) dissipated by the fluid is simply related to the stress tensor σ_{ij} and flow u_i in the suspension:

$$W = \frac{1}{V_0}\int_{V_0}\frac{1}{2}(\partial_j u_i)(\sigma_{ij}+\sigma_{ji})\mathrm{d}V\,. \tag{19}$$

For dilute suspensions of torque- and force-free particle, the above relation becomes[8]

$$W = \frac{1}{2}A^{\infty}_{ij}(\bar{\sigma}_{ij}+\bar{\sigma}_{ji})\,, \tag{20}$$

where $\bar{\sigma}_{ij}$ stands for the components of the average stress field in the suspension, equal to the stress tensor averaged with the steady-state distribution $P(\mathbb{R},\infty)$ obtained with the Langevin equation (16). The suspension stress field is, to the first order approximation of volumetric concentration c, equal to the Newtonian ambient stress σ^{∞}_{ij} plus a disturbance field due to the particle presence:

$$\bar{\sigma}_{ij} = \sigma^{\infty}_{ij} + \eta c\int(C_{ijkl}S^{\infty}_{kl}+6DF_{ij})P(\mathbb{R},\infty)\mathrm{d}\mathbb{R}\,. \tag{21}$$

By recalling the explicit definition of the ambient shear flow, the viscosity of the suspension η' is

$$\eta' = \eta\left(1+c\int\left(C_{1212}+6\mathrm{Pe}^{-1}F_{12}\right)P\left(\mathbb{R},\infty\right)\mathrm{d}\mathbb{R}\right)\,, \tag{22}$$

from which we define the intrinsic viscosity

$$[\eta] = \lim_{c\to\infty}\frac{1}{c}\left(\frac{\eta'}{\eta}-1\right) = \int\left(C_{1212}+6\mathrm{Pe}^{-1}F_{12}\right)P\left(\mathbb{R},\infty\right)\mathrm{d}\mathbb{R}\,. \tag{23}$$

Let the relative intrinsic viscosity be defined as the intrinsic viscosity normalized by its zero-shear value[9]

$$[\eta]_r = \frac{[\eta]}{[\eta]\,|_{\mathrm{Pe}=0}}\,. \tag{24}$$

The particles contribute to the average stress tensor through an indirect and a direct contribution. The indirect contribution arises from the deformation of the flow produced by the particles, and is embodied by the orientation- and shape-dependent tensor $\mathbb{C}$. Its components are[8]:

$$C_{ijkl} = \frac{J_1(R_{i1}R_{j1}-\frac{1}{3}\delta_{ij})(R_{k1}R_{l1}-\frac{1}{3}\delta_{kl})}{\frac{1}{4}(J_1J_2+J_2J_3+J_3J_1)} + \frac{(R_{i2}R_{j3}+R_{i3}R_{j2})(R_{k2}R_{l3}+R_{k3}R_{l2})}{\frac{1}{2}I_1}+\cdots\,, \tag{25}$$

with four similar terms obtained with cyclic permutations of the numeric indices. I_i and J_i, defined in Appendix C, are elliptic integrals used to describe the flow past an ellipsoid. The direct contribution comes from the fact that the diffusion process gives rise to an "effective Brownian angular velocity" (see (13)). Ref. [14] showed that this contribution can be described with a tensor $\mathbb{F}$ with components

$$F_{ij} = (\frac{K-\Lambda}{K\Lambda-1}-\Lambda)R_{i1}R_{j1}+(K+\frac{\Lambda-K}{K\Lambda-1})R_{i2}R_{j2}-(K+\Lambda)R_{i3}R_{j3}\,. \tag{26}$$

For a suspension of spheres, $F_{ij}=0$, $P(\mathbb{R},\infty)=\frac{1}{8\pi^2}$ and $C_{1212}=\frac{5}{3}(R^2_{11}R^2_{21}+R^2_{12}R^2_{22}+R^2_{13}R^2_{23})+\frac{5}{2}\left[(R_{12}R_{23}+R_{13}R_{22})^2+(R_{13}R_{21}+R_{11}R_{23})^2+(R_{11}R_{22}+R_{12}R_{21})^2\right]$ the formula for the intrinsic viscosity becomes

Check numerically (27)

$$[\eta] = \frac{1}{8\pi^2}\int C_{1212}\sin(\theta)\mathrm{d}\theta\mathrm{d}\phi\mathrm{d}\psi = \frac{5}{2}\,. \tag{27}$$

Such suspensions exhibit a higher viscosity than that of the suspending fluid[1,2] because of the energy dissipation of the stresses at the particle's surface, with an intrinsic viscosity of $[\eta] = 5/2$. This value is a minimum because the spherical shape is associated with a minimum energy dissipation.

Reference

Axisymmetric particles give rise to a viscosity higher than that of spheres because of their shape: sharp ends and edges determine a higher disturbance in the flow, which is in turn related to higher stresses at the particle's surface. The shape dependence of the stresses is embodied by the orientation-dependent material tensors $\mathbb{C}$ (and $\mathbb{F}$) in (23). Moreover it is apparent from the first term of eq. (23) that the intrinsic viscosity of non-spherical particles can have a shear dependency: it is known that solutions of axisymmetric ellipsoids exhibit shear-thinning behaviour, i.e. the solution's viscosity decreases monotonically when a stronger shear is applied[11]. The viscosity has two constant limiting values at vanishing and dominant shear. Departure from the limits is linear. It was shown[12] that the plateaux are reached when the Péclets number is either much greater or smaller than $\lambda^3 + \lambda^{-3}$. At high shear rates the plateau's height depends on the particle's aspect ratio: for suspensions of rods the limiting value increases proportionally to $\lambda/\ln\lambda$. Conversely, suspensions of infinitely thin disks reach a litimiting value $[\eta] \approx 3.13$. In the limit of vanishing shear the viscosity is linearly proportional to Pe: the suspension behaves like a quasi-Newtonian fluid with viscosity higher than that of the suspending fluid. The additional viscosity is proportional to $\lambda^2/\ln\lambda$ for rods and λ^{-1} for disks[12] of extreme particle aspect ratio.

The rheology of suspensions of asymmetric ellipsoids is comparatively little studied. Low shear values were found with both numerical[14] and analytical approaches[15]. Similarly to symmetric ellipsoids, the suspension was found to behave like a quasi-Newtonian fluid, with intrinsic viscosity proportional to the Péclet number[15] by means of a linear perturbation expansion in Pe. The zero-shear limiting value of viscosity has a strong dependence on particle geometry: for long asymmetric rods ($\lambda \to \infty$) it is $\propto \lambda^2/\kappa\ln\lambda$, while for asymmetric thin disks ($\lambda \to 0$) it is proportional to $1/\kappa\lambda\ln\lambda$.

found it in Haber-Brenner, must implement it

III. RESULTS

In the absence of thermal noise, the dynamics of a triaxial ellipsoid are entirely defined by the hydrodynamic angular velocity (2). The inherent nonlinear dependency of this quantity on the particle orientation makes the tumbling dynamics complicated with features of quasi-periodicity[5] and chaos[6]. Adding Brownian noise to the dynamics results in a probability distribution in the space of orientations, which in turns affects the rheological properties of the suspension. In this section we show numerical results concerning the steady-state orientation distribution obtained with the Langevin simulation, and the intrinsic viscosity of a dilute suspension of ellipsoids as a function of particle aspect ratio and noise strength. In this work we use the (Z-Y'-X") convention[16]: given an initial frame of reference where the particle's $(\boldsymbol{n}, \boldsymbol{p}, \boldsymbol{q})$ axes are aligned with the laboratory frame $(\boldsymbol{x}, \boldsymbol{y}, \boldsymbol{z})$, the particle is rotated around $\boldsymbol{q}$ by and angle ϕ, then around the rotated axis $\boldsymbol{p}$ by θ and finally around $\boldsymbol{n}$ by ψ.

The particle's major axis $\boldsymbol{n}$ always performs a positive rotation around the direction of vorticity, tumbling end to end. Between each flip the axis $\boldsymbol{n}$ can be found perpendicular to the flow direction. In terms of Euler angles this happens when $\phi = n\pi/2$. It is therefore possible to define a Poincaré surface of section as the intersection between the trajectory of the particle in the Euler space and the plane perpendicular to the flow direction. Each point on the surface of section has two components: one is the projection of the major particle axis onto the vorticity direction i.e. $\cos\theta = \boldsymbol{n}.\boldsymbol{z}$ and the other is the particle's intrinsic rotation ψ. Similarly we slice the orientational distribution along the flow direction and the elongating and compressing strain directions, respectively $\phi = 0$ and $\phi = \pi/4\,, 3\pi/4$.

A. Particle dynamics

In this section we describe the steady-state orientational distribution $P(\psi, \cos\theta | t \to \infty)$, sliced at different ϕ i.e. in different directions, for an asymmetric ellipsoid ($\lambda = 10, \kappa = 5$) in several noise regimes. Each row corresponds to a different slice: first row is sliced in flow direction $\phi = 0$, then elongating strain, perpendicular to flow, and finally compressing strain. The Poincaré surface of section of the deterministic dynamics is shown in the first column. In the second and third columns we show the orientational distribution at different noise strengths, Pe The distribution is plotted as a linearly color coded heat map.

Describe distribution along flow and strain directions

The distribution in the direction perpendicular to the flow bears little resemblance to the deterministic surface of section, even for low noise levels. Perhaps the biggest similarity lies in the corners of the pictures: the distribution has a peak at position $\cos\theta = 1, \psi = \pi/2$ (and at three more locations due to inherent symmetries of the joint particle-flow system[5]), whereas the SOS shows a considerable concentration of points in the same position, well within the stochastic layer. The integrable regions (tori) cannot be discerned in the distribution, and seem to be associated with a relative minimum probability. The distribution is affected by noise: at Pe = 1 (panel c3) the distribution starts becoming "flatter" (smaller gradients). Eventually the distribution becomes so flat as to be almost uniform. With the data obtained so far it can't be conclusively ruled whether the distribution approaches the uniform case in the limit Pe $\to 0$ as a symmetric particle or, conversely, if some features of anisotropy (viz. a structure depending on ψ) are retained.
The distribution at the surface of section has limited effects on the rheological properties of the suspension: particles subject to strong shear are observed most of the time with their major axis aligned with the flow, whence most of the contribution to viscosity comes.

B. Rheological properties

In Figure 3 we show the intrinsic viscosity of a dilute suspension of tri-axial ellipsoids with several primary aspect ratio λ, as a function of the secondary aspect ratio spanning $\kappa \in [1, \lambda]$ for different noise regimes. Data obtained with the Langevin simulation here introduced show excellent agreement with previous theoretical results obtained in the zero-shear limit for asymmetric ellipsoids[15]. Slightly elongated and prolated ellipsoids (same figure, top-left panel) show a weak shear thinning behaviour. The viscosity has maxima at $\kappa = 1$ and $\kappa = \lambda$, i.e. axisymmetric particle shapes, and a relative minimum in between whose position depends on Pe. The curve is slightly asymmetric: short rods of aspect ratio λ have higher viscosity than disks with aspect ratio $1/\lambda$. The intrinsic viscosity reaches a limiting value when Pe $\to \infty$, slightly higher than that of spheres. his value is almost independent of particle shape.
Increasing the aspect ratio λ has several effects: the zero-shear intrinsic viscosity increases. This effect is more pronounced for rods than for disks, leading to an asymmetrical viscosity curve. At the other end, zero-noise viscosity also increases, yet remains close to the value for suspensions of spherical particles. At vanishing noise, the intrinsic viscosity is very weakly dependent on particle shape: the curve has a maximum at $\kappa = 1$, and a lower one at $\kappa = \lambda$, with a plateau in between.
In Figure 4 we show the relative intrinsic viscosity as function of Pe for particles of fixed λ and several κ. The zero shear value used for the normalization is that analytically obtained by Ref. [15]. Previous results obtained for axisymmetric particles in finite[11] and vanishing noise[12] are shown respectively with crosses and dashed lines. Solid lines are our results obtained with langevin simulations.

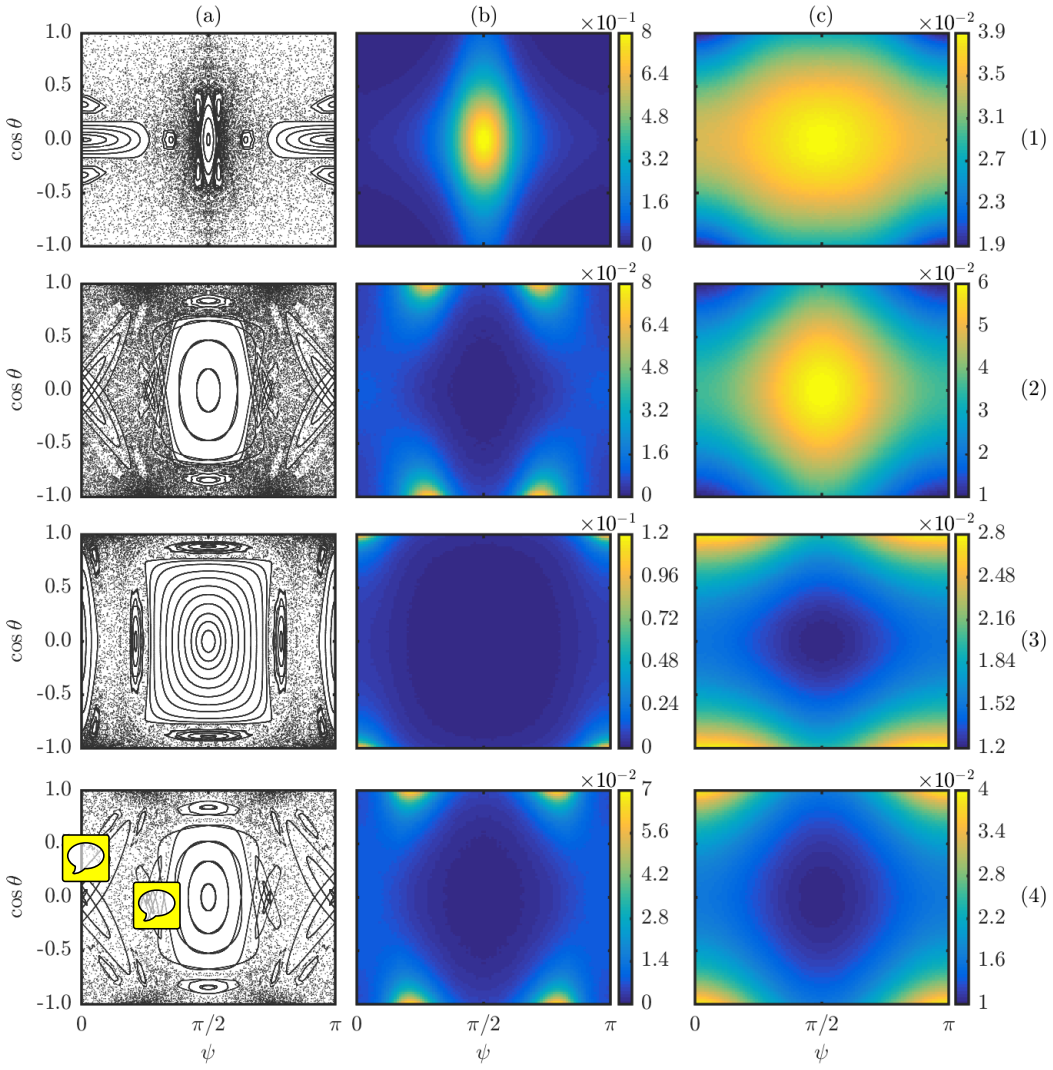

FIG. 2. Surface of section (column (a)) and steady-state distribution $P(\psi, \cos\theta, t \to \infty)$ (heat maps) in direction of flow respectively elongating strain, perpendicular to flow and compressing strain ($\phi = 0, \pi/2, \pi, 3\pi/2$ in rows (1) to (4)) for an asymmetric ellipsoid ($\lambda = 10$, $\kappa = 5$) immersed in a simple shear flow with increasing Brownian noise ($\mathrm{Pe} = 10^2, 10^0$ columns (b) and (c)).

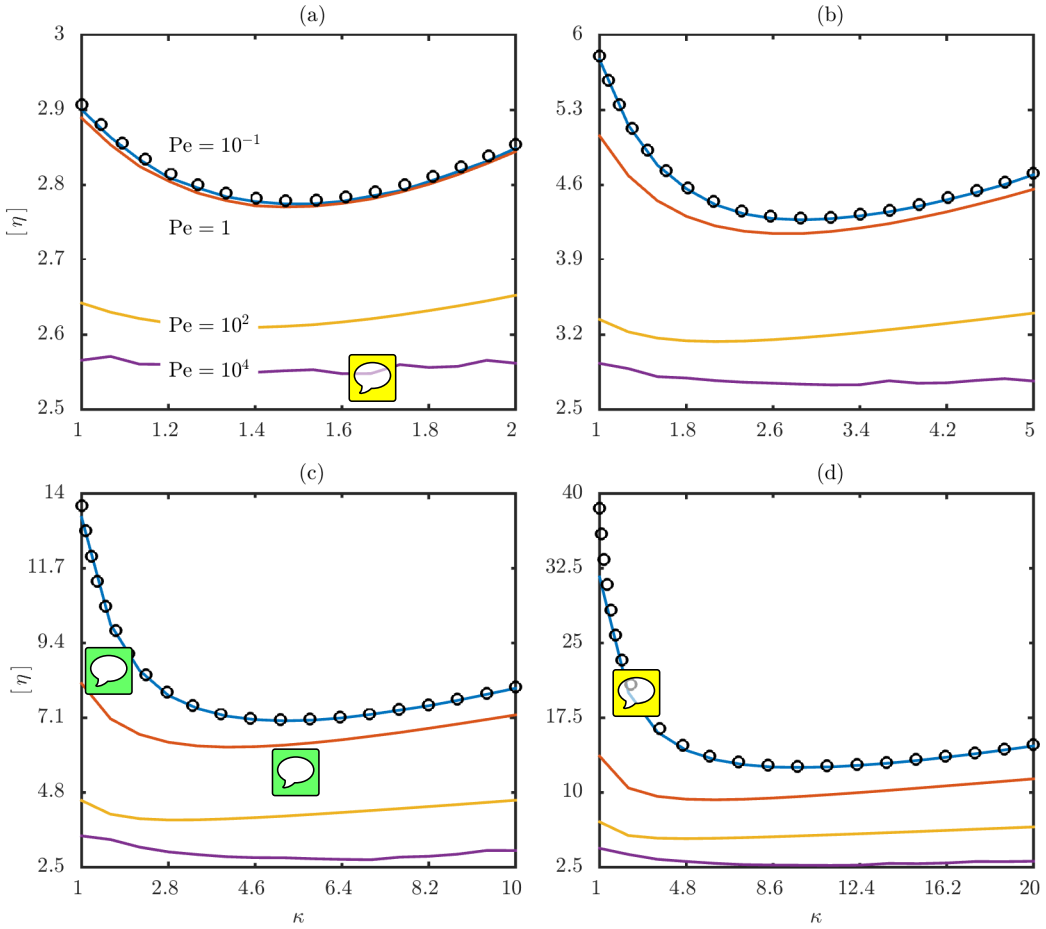

FIG. 3. Intrinsic viscosity (solid lines) of triaxial ellipsoids as a function of κ. Data in each panel is produced for particles of different primary aspect ratio λ: in panel (a) $\lambda = 2$, panel (b) $\lambda = 5$, panel (c) $\lambda = 10$, panel (d) $\lambda = 20$. κ spans from rods to disks, i.e. $\kappa \in [1, \lambda]$. Each solid line has a fixed noise strength Pe, as indicated in the panel (a). Solid lines of same color across different panels have the same noise strength. Black $\circ$ data are theoretical results for asymmetric particles in vanishing shear[15]. Add finite [12] and vanishing[11] noise results for symmetric particles shown in Fig. 4?

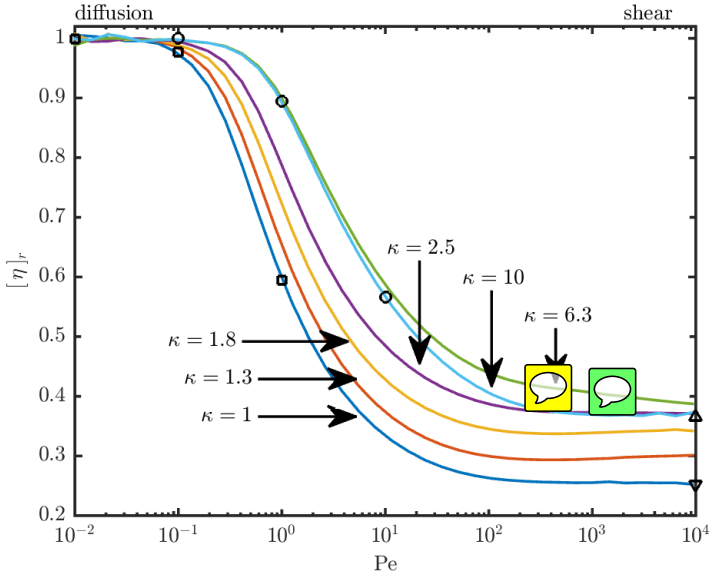

FIG. 4. Relative intrinsic viscosity (intrinsic viscosity normalized by its corresponding zero-shear intrinsic viscosity[15]) of triaxial ellipsoids as a function of Pe. Model parameters are $\lambda = 10$ and several values of κ marked on figure. Symbols mark previous results for axisymmetric particles obtained in finite[11] (circles and squares) and vanishing noise[12] (up- and down-triangles) regimes are marked with symbols.

IV. CONCLUSIONS

Asymmetric ellipsoids mostly driven by the shear flow tend to spend most of the time with their major axis aligned with the flow direction and their intermediate axis aligned with the vorticity, in a edge-on configuration. The particle occasionally flips on itself around its minor axis between the two stable positions of alignment with the flow. Moderately asymmetric particles flip in several distinct modes: one "edge-on" mode is with the major axis aligned with the vorticity and intermediate axis in the flow direction. Several other distinct modes can be observed: typically the particle flips edge on with its major axis tilted about the flow direction in what can be called a "tilted edge-on" mode.
Dilute suspensions of asymmetric ellipsoids show a shear thinning behaviour similar to that of symmetric particles. The viscosity decreases because as the shear is stronger the particles tend to align themselves with the flow, in a low-stress configuration. In the low noise regime the intrinsic viscosity reaches a limiting value comparable to that of suspensions of hard spheres. This value is nearly independent on the shape of the particle, even though particle dynamics is extremely sensitive on asymmetry[17]. Experimental confirmation is needed to validate this finding. The onset of the low noise plateau depends on the the aspect ratios of the particle. While the functional form is as of this date unkown, it is expected to be similar to that of symmetric particles[13].

[1] A. Einstein, "Eine neue Bestimmung der Moleküldimensionen," Ann. Phys. (1906).
[2] A. Einstein, "Berichtigung zu meiner Arbeit: Eine neue Bestimmung der Moleküldimensionen," Ann. Phys. (1911).
[3] H. Brenner, "Coupling between the translational and rotational Brownian motions of rigid particles of arbitrary shape - II. General theory," J. Coll. Int. Sc (1967).
[4] G. B. Jeffery, "The Motion of Ellipsoidal Particles Immersed in a Viscous Fluid," Proc. R. Soc. A **102**, 161–179 (1922).
[5] E. J. Hinch and L. G. Leal, "Rotation of small non-axisymmetric particles in a simple shear flow," J. Fluid Mech. **92**, 591–608 (1979).

[6]A. L. Yarin, O. Gottlieb, and I. V. Roisman, "Chaotic rotation of triaxial ellipsoids in simple shear flow," J. Fluid Mech. **340**, 83–100 (1997).
[7]F. Perrin, "Mouvement brownien d'un ellipsoide (I). Dispersion diélectrique pour des molécules ellipsoidales," Le journal de physique et Le radium (1934).
[8]G. K. Batchelor, "The stress system in a suspension of force-free particles," J. Fluid Mech. (1970).
[9]S. Kim and S. J. Karrila, *Microhydrodynamics: principles and selected applications*, Butterworth-Heinemann series in Chemical Engineering (Butterworth-Heinemann, Boston, 1991).
[10]R. Simha, "The influence of Brownian movement on the viscosity of solutions," J. Phys. Chem (1940).
[11]H. A. Scheraga, "Non-Newtonian viscosity of solutions of ellipsoidal particles," J. Chem. Phys. (1955).
[12]E. J. Hinch and L. G. Leal, "The effect of Brownian motion on the rheological properties of a suspension of non-spherical particles," Journal of Fluid Mechanics **52**, 683–712 (1972).
[13]L. G. Leal and E. J. Hinch, "The effect of weak Brownian rotations on particles in a shear flow," J. Fluid Mech. (1971).
[14]J. M. Rallison, "The effects of Brownian rotations in a dilute suspension of rigid particles of arbitrary shape," J. Fluid Mech. (1978).
[15]S. Haber and H. Brenner, "Rheological properties of dilute suspensions of centrally symmetric Brownian particles at small shear rates," Journal of Colloid and Interface Science (1984).
[16]H. Goldstein, *Classical Mechanics* (Addison-Wesley, Reading, Massachusetts, 1980).
[17]J. Einarsson, A. Johansson, S. K. Mahato, Y. N. Mishra, J. R. Angilella, D. Hanstorp, and B. Mehlig, "Periodic and aperiodic tumbling of microrods advected in a microchannel flow," Acta Mech **224**, 2281–2289 (2013).
[18]A. Oberbeck, "Über stationäre Flüssigkeitsbewegungen mit Berücksichtigung der inneren Reibung," J. reine angew. Math. (1876).
[19]N. G. V. Kampen, *Stochastic Processes in Physics and Chemistry* (Elsevier Science Publishers, 1981).
[20]L. H, *Hydrodynamics* (Cambridge: University Press, 1895).

Appendix A: Quaternions

- Define quaternions
- Eq. of motion
- Conversion to Rot matrix and Euler angles

Appendix B: Fokker-Planck equation

- Schematic description of Van Kampen's method for deriving F-P from microscopic dynamics
- Derivation of F-P for quaternions (and rotation matrices?)
- Langevin eq. and integration scheme for quaternions

Appendix C: Brownian angular velocity statistics

The mobility tensor is diagonal when expressed in particle frame and has components

$$M_{11} = 3/2(J_1 + 2I_1 a_2^2 a_3^2/(a_2^2 + a_3^2))\,. \tag{C1}$$

Its two remaining components are obtained with cyclic permutations of the indices. J_i and I_i are elliptical integrals[8] of the form

$$J_1 = a_1 a_2 a_3 \int_0^\infty \frac{(a_2^2 + a_3^2)\mathrm{d}\xi}{[(a_1^2+\xi)(a_2^2+\xi)(a_3^2+\xi)]^{1/2}(a_2^2+\xi)(a_3^2+\xi)}\,, \tag{C2a}$$

$$I_1 = a_1 a_2 a_3 \int_0^\infty \frac{\xi\mathrm{d}\xi}{[(a_1^2+\xi)(a_2^2+\xi)(a_3^2+\xi)]^{1/2}(a_2^2+\xi)(a_3^2+\xi)}\,. \tag{C2b}$$

The four remaining integrals are obtained by cyclic permutations of the indices. These quantities arise in the calculation of the flow past an ellipsoid[20].

Here: say what the meaning of J_i and I_i is (particle geometry). relation to moments of inertia? relation to appendix of jonas recent phys. fluids paper on axisymmetric particles.

Appendix D: Particle dynamics?

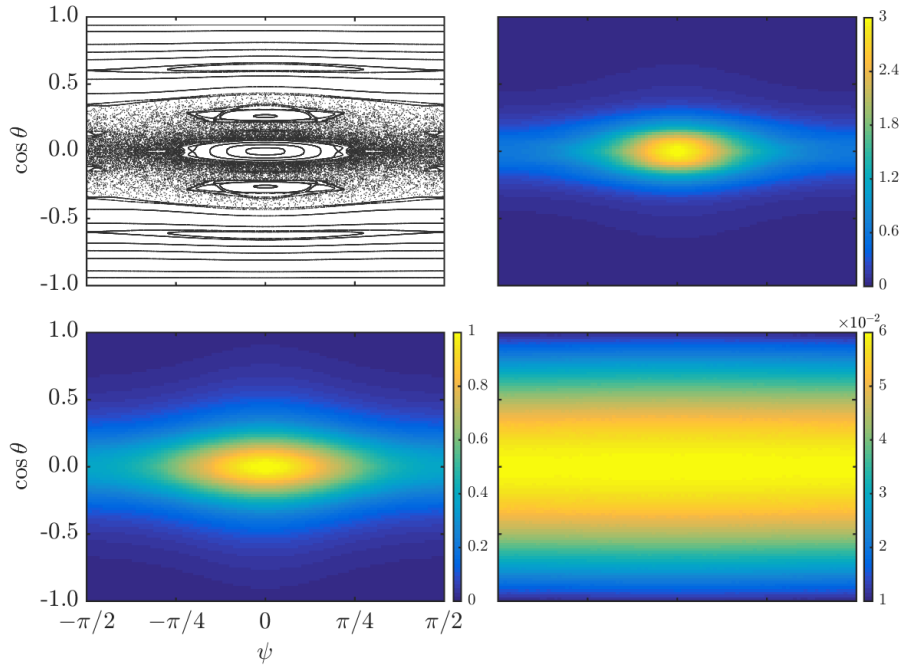

FIG. 5. Poincaré surface of section (top) and distribution (heat map) over the flow direction $P(\psi, \cos\theta \,|\, \phi = 0)$ for an asymmetric ellipsoid ($\lambda = 10$, $\kappa = 1.5$) immersed in a simple shear flow with increasing Brownian noise ($\mathrm{Pe} = 10^4, 10^2, 10^0$ from second to last row).

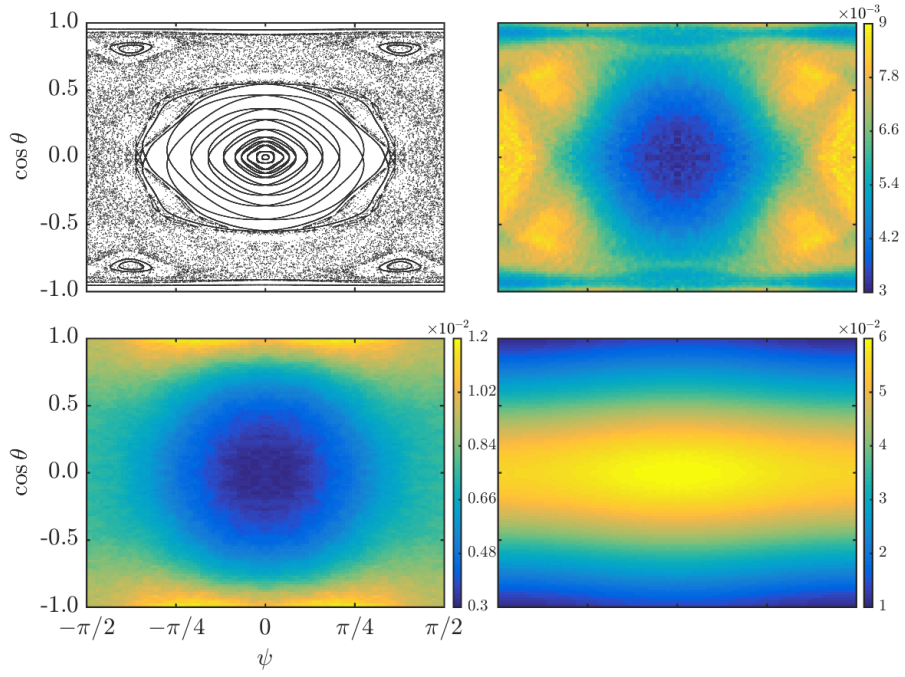

FIG. 6. Poincaré surface of section (top) and distribution (heat map) over the strain direction $P(\psi, \cos\theta \,|\, \phi = \pi/4)$ for an asymmetric ellipsoid ($\lambda = 10$, $\kappa = 1.5$) immersed in a simple shear flow with increasing Brownian noise ($\mathrm{Pe} = 10^4, 10^2, 10^0$ from second to last row).

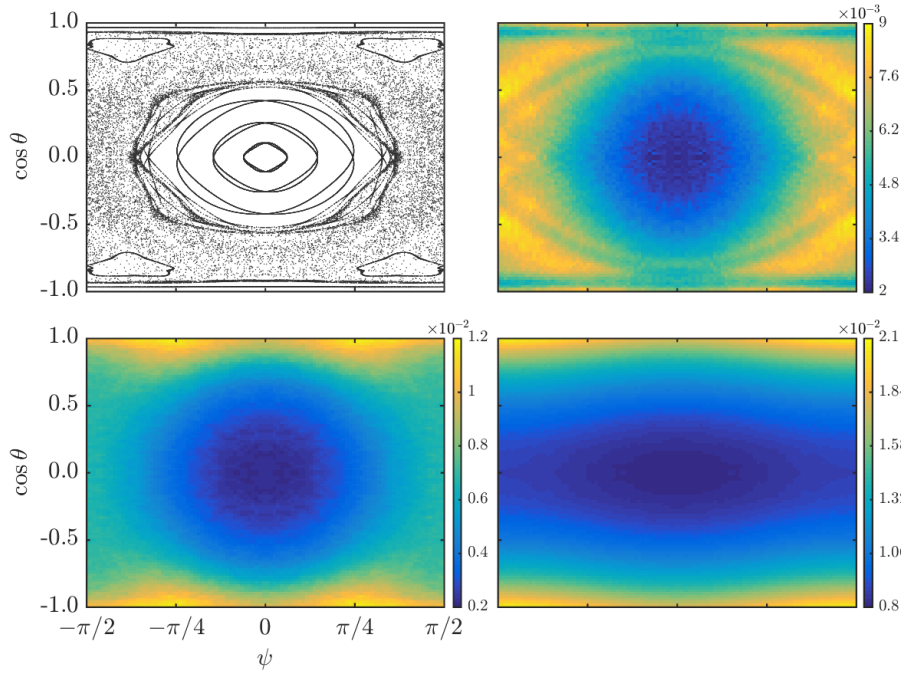

FIG. 7. Poincaré surface of section (top) and distribution (heat map) over the secondary strain direction $P(\psi, \cos\theta \,|\, \phi = 3\pi/4)$ for an asymmetric ellipsoid ($\lambda = 10$, $\kappa = 1.5$) immersed in a simple shear flow with increasing Brownian noise ($\mathrm{Pe} = 10^4, 10^2, 10^0$ from second to last row).

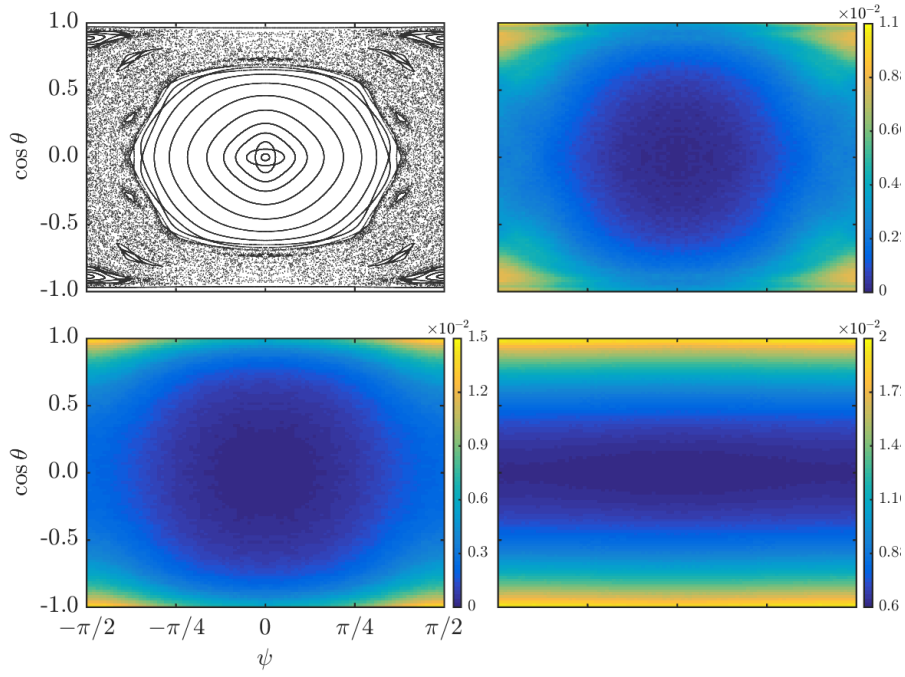

FIG. 8. Poincaré surface of section (top) and distribution (heat map) over the Poincaré surface of section $P(\psi, \cos\theta \,|\, \phi = \pi/2)$ for an asymmetric ellipsoid ($\lambda = 10$, $\kappa = 1.5$) immersed in a simple shear flow with increasing Brownian noise ($\mathrm{Pe} = 10^4, 10^2, 10^0$ from second to last row).